# Climate change and forest fires synergistically drive widespread melt events of the Greenland Ice Sheet

Kaitlin M. Keegan[a,1], Mary R. Albert[a], Joseph R. McConnell[b], and Ian Baker[a]

[a]Thayer School of Engineering, Dartmouth College, Hanover, NH 03755; and [b]Desert Research Institute, Nevada System of Higher Education, Reno, NV 89512

Edited by Robert E. Dickinson, The University of Texas at Austin, Austin, TX, and approved May 1, 2014 (received for review March 23, 2014)

**In July 2012, over 97% of the Greenland Ice Sheet experienced surface melt, the first widespread melt during the era of satellite remote sensing. Analysis of six Greenland shallow firn cores from the dry snow region confirms that the most recent prior widespread melt occurred in 1889. A firn core from the center of the ice sheet demonstrated that exceptionally warm temperatures combined with black carbon sediments from Northern Hemisphere forest fires reduced albedo below a critical threshold in the dry snow region, and caused the melting events in both 1889 and 2012. We use these data to project the frequency of widespread melt into the year 2100. Since Arctic temperatures and the frequency of forest fires are both expected to rise with climate change, our results suggest that widespread melt events on the Greenland Ice Sheet may begin to occur almost annually by the end of century. These events are likely to alter the surface mass balance of the ice sheet, leaving the surface susceptible to further melting.**

The massive Greenland Ice Sheet (GIS) experiences annual melting at low elevations near the coastline. However, surface melt is extremely rare over ~600,000 km$^2$ of the "dry snow region" in its center (1). In July 2012, ground-based observations confirmed indications from satellite imagery that, for several days, surface melt had occurred over 97% of the ice sheet's surface (Fig. 1) (2). Melting in the dry snow zone does not contribute to sea level rise; instead, water from these events percolates into the snowpack and refreezes (3). Subsequently, it was determined that the radiative effects of a thin layer of low-level 'liquid clouds" added to warming conditions over the GIS in 2012 (4). Evidence from firn cores collected at multiple sites demonstrated that the most recent previous spatially extensive melt occurred in 1889. Thus, at present, widespread melt events are anomalous.

Interestingly, although 1889 and 2012 were relatively warm years, there have been even warmer years over the past century when the snow in the coldest part of the ice sheet did not melt. As such, we hypothesized that, in addition to relatively warm temperatures, the snow albedo may also play a critical role in inducing melt in the dry snow region. In this paper we evaluate the causes of both the 1889 and the 2012 melt events and estimate the expected frequency of these events in the context of continuing climate change in the Arctic.

## Results and Discussion

Ice layers formed from refrozen snowmelt in porous firn are prominent upon visual inspection. A prominent ice layer dated to 1889 in multiple firn cores from central Greenland (5–7) and northwest Greenland (8) has been briefly mentioned in the literature. It has been traditionally thought that these melt layers were likely part of a widespread melt event in 1889, but the extent of the melt was unknown. Here, we present physical evidence of a melt layer dating to 1889 in six additional Greenland firn cores from four sites: Summit, NEEM, D4, and ACT 3 (Fig. S1 and Table S1). Thus, the 1889 melt event appears to have been very widespread, and included the dry snow region.

During most summers in the 20th and 21st centuries, it has been too cold to permit snowmelt in the dry snow region of the GIS. Accordingly, the widespread melting in 1889 and in 2012 occurred during periods that were unusually warm (Fig. 2). We used firn core records of stable water isotopes, $\delta^{18}O$, as a proxy for temperature (9), although it should be noted that there was only a moderate correlation ($r^2 = 0.29$, Fig. S2) between temperature and $\delta^{18}O$ at Summit from 2000 to 2010. As methods for the indirect estimation of temperature improve, more accurate historical temperature records may become available. Nevertheless, these data suggest that 1889 was a particularly warm year (Fig. 2*C*). However, this was not the warmest year recorded in the firn. Temperatures were warmer in 1785, for example, but melting in the dry snow region did not occur in that year (Fig. 2*A*). Similarly, widespread melting in the dry snow region did not occur during the most recent record-breaking melt extent years of 2002, 2007, or 2010 (10–12). Thus, high temperatures alone are often not enough to cause widespread melt. Indeed, continuous measurements of near-surface conditions at Summit Station from the Greenland Climate Network (GC-Net) instruments show that the temperature reached 0 °C on July 12, 2012 (13), providing ~0.94 MJ m$^{-2}$ of energy, although ~1.1 MJ m$^{-2}$ of energy is needed to cause melting in the accumulation area of the ice sheet (calculated in *SI Materials and Methods*). Under present conditions in the dry snow region, this energy threshold cannot be attained from the average summer temperature, irradiance, and albedo. Despite melting in the ablation zone of the ice sheet during summer, unusually warm conditions have not been sufficient to cause widespread melting into the dry snow region.

The albedo of snow is an important factor in snowmelt. If temperatures at the surface of the ice sheet are warm and snow is allowed to age in the absence of fresh accumulation, it will coarsen, and this changing morphology can lower the albedo by up to 14% (14). In addition, black carbon (BC) from incomplete fossil fuel combustion or biomass burning can reach the top of the ice sheet and reduce the albedo by up to 7% (15, 16). We measured BC on a Summit shallow core and also on a near-surface sample of firn containing the 2012 melt layer with an

### Significance

**Through an examination of shallow ice cores covering a wide area of the Greenland Ice Sheet (GIS), we show that the same mechanism drove two widespread melt events that occurred over 100 years apart, in 1889 and 2012. We found that black carbon from forest fires and rising temperatures combined to cause both of these events, and that continued climate change may result in nearly annual melting of the surface of the GIS by the year 2100. In addition, a positive feedback mechanism may be set in motion whereby melt water is retained as refrozen ice layers within the snow pack, causing lower albedo and leaving the ice sheet surface even more susceptible to future melting.**

Author contributions: K.M.K. designed research; K.M.K. and J.R.M. performed research; K.M.K., M.R.A., J.R.M., and I.B. analyzed data; and K.M.K., M.R.A., and I.B. wrote the paper.

The authors declare no conflict of interest.

This article is a PNAS Direct Submission.

Freely available online through the PNAS open access option.

[1]To whom correspondence should be addressed. E-mail: kaitlin.m.keegan.th@dartmouth.edu.

This article contains supporting information online at www.pnas.org/lookup/suppl/doi:10.1073/pnas.1405397111/-/DCSupplemental.

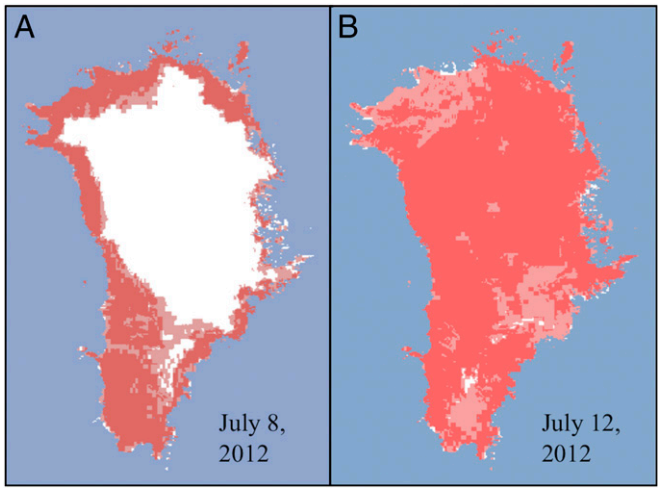


**Fig. 1.** Melt extent over the GIS determined from Oceansat-2 satellite scatterometer, Special Sensor Microwave Imager/Sounder, and Moderate-resolution Imaging Spectroradiometer satellite data for (*A*) July 8, 2012, and (*B*) July 12, 2012. Red areas indicate melt detected by the satellites, white areas indicate no melt, and blue represents ocean. The surface of almost the entire ice sheet, including the dry snow region, experienced melt on July 12, 2012. Figure courtesy of Dorothy Hall, NASA Goddard Space Flight Center.

inductively coupled plasma mass spectrometry (ICP-MS) continuous flow analysis system. This included measurements of total BC concentrations, as well as ammonium, $\delta^{18}O$, and a suite of other measurements that were used to establish the depth–age scale. The presence of a high concentration of ammonium concurrent with the BC indicates that the source of the BC was large boreal forest fires (17). Since BC coeval with high concentrations of non-sea-salt sulfur (nss-S) indicates a fossil fuel source of BC (18), we consider low nss-S concentrations concurrent with BC another indication of a forest fire source.

The total BC concentration varies inter- and intra-annually in the firn. The annual average BC concentration was 1.7 ng $g^{-1}$ during the preindustrial period (1750–1850 A.D.), 4.0 ng $g^{-1}$ during the early industrial period (1851–1950), and 2.3 ng $g^{-1}$ from 1951 to present (Fig. 2). Over our 262-y record, there are four large spikes in the annual average BC concentration of 10.4, 10.4, 14.3, and 14.4 ng $g^{-1}$ in 1868, 1889, 1908, and 2012, respectively (Fig. 2). Visual inspection of the firn core revealed the presence of an ice layer in 1889, and surface samples contained a melt layer formed in 2012, but not in 1868 or 1908 when equivalent or greater BC spikes occurred. The low $\delta^{18}O$ indicates that temperatures were too cool to permit melt during in 1868 as well (Fig. 2*B*). Similarly, while a spike in BC in 1908 was likely due to forest fires, indicated by a high ammonium concentration, analysis of the stratigraphy suggests that it was deposited late in the year (Fig. 2*D*). Thus, it was likely deposited at a time when the available surface energy was well below the threshold for melt. Despite the reduced albedo from the BC, temperatures would not have been warm enough to permit melt during that time. Lastly, despite the warm temperature in 1785 indicated by a high $\delta^{18}O$, a melt event did not occur, because of the lack of albedo reduction from BC (Fig. 2*A*). The absence of nss-S further implicates the forest fire origin of the BC and concurrent ammonium in 1868, 1889, and 1908 (Fig. S3), because presence of nss-S indicates a fossil fuel source for BC (18).

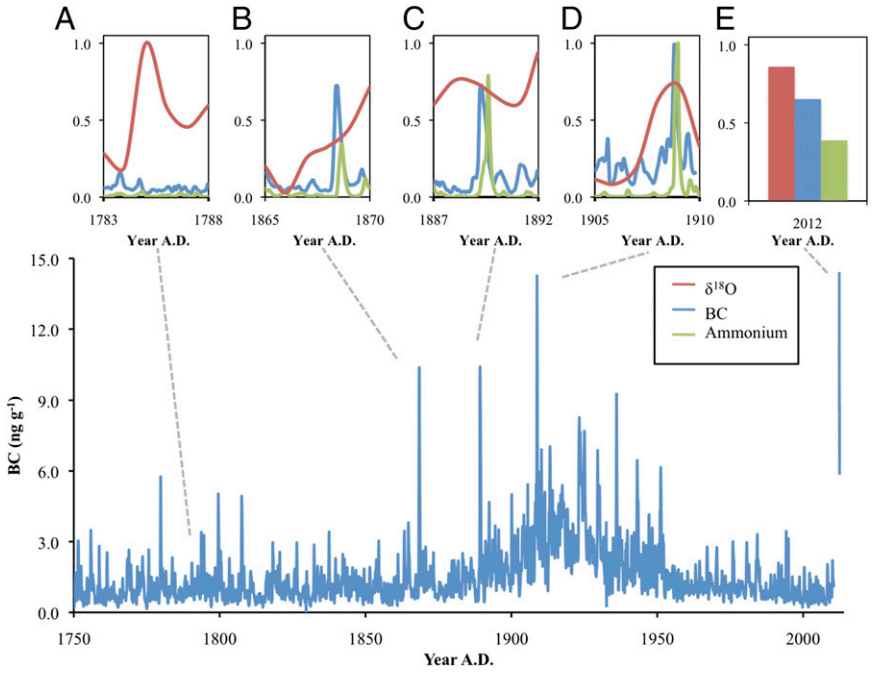


**Fig. 2.** (*Lower*) The annual average BC concentrations (ng $g^{-1}$) from 1750 to 2010 of the Summit-2010 firn core and the 2012 surface section. (*Upper*) Sections of the BC record along with $\delta^{18}O$ and ammonium records, plotted on a relative scale normalized to the maximum and minimum values in each record, for the time intervals (*A*) 1783–1788, (*B*) 1865–1870, (*C*) 1887–1892, and (*D*) 1905–1910, as well as (*E*) the normalized average value of BC and ammonium concentrations from the July 2012 surface sample, and approximate $\delta^{18}O$. These time intervals demonstrate extreme scenarios in the center of the GIS with (*B*–*E*) depicting the highest concentrations of BC, and (*A*) the warmest temperature since 1750, but widespread melt events only occurred in 1889 and 2012. In *C* and *E*, melt occurred because of the deposition of high concentrations of BC and ammonium, indicating an albedo reduction due to BC from summer forest fires. Importantly, these deposition events occurred during warm summers. In *B*, a high concentration of BC and presence of ammonium during a cooler summer suggest that the surface was below the energy threshold for melt. In *D*, the highest concentrations of BC and ammonium in the record were recorded during an average summer, suggesting that the BC was deposited at a time of the year when the available surface energy was well below the threshold for melt. The warmest temperature recorded in the core occurred in 1785, but widespread melting did not occur due to low BC concentration.

Unlike other years where BC peaks occurred but melting of the ice sheet was minimal, widespread melting of the entire GIS surface did occur in 1889 and 2012. Why did it occur in these years and not the others? Our data suggest that during these two years, abnormally warm summer temperatures combined with BC deposited on the ice sheet to reduce albedo below a critical threshold. In 1889, the high BC (10.4 ng $g^{-1}$) and ammonium (7.0 μM) concentrations observed in firn cores indicate that the source of BC was forest fires (Fig. 2*C* and Fig. S3). Indeed, biomass burning due to large forest fires was documented in 1889 (19, 20). Further, analysis of the BC particles is necessary to fingerprint a specific geographic source of these deposits, and is beyond the scope of this study. However, air mass back-trajectories before the 2012 melting event show sources ranging from Siberia to North America (Fig. S4). Moreover, measurements of $\delta^{18}O$ (−32.4 ‰) demonstrate that this BC deposition occurred during an anomalously warm summer (Fig. 2*C* and Fig. S3). Similarly, in July 2012, the surface of the ice sheet experienced unusually warm temperatures, enhanced by a thin layer of low-level liquid clouds (3), that averaged −1.9 °C, and exceeded 0 °C for ∼5 min, on July 12 (13). Concurrently, BC was deposited with an ammonium signature (6.1 μM) indicating a forest fire source (Fig. S3), originating from the significant forest fires in Siberia (21) and North America in late June and July 2012 (22, 23) that were transported to Summit in early July (Fig. S4). The albedo reduction (∼6%) caused by warming and BC presence (14, 16) on July 12, 2012, at Summit provided an extra 0.3 MJ $m^{-2}$ of energy to the surface, pushing the surface energy balance over the threshold of 1.1 MJ $m^{-2}$ for melting. Therefore, changes in albedo due to BC deposition from Northern Hemisphere forest fires together with unusually warm conditions were the driving factors in the extensive 1889 and 2012 melt events across the ice sheet.

Over the next century, climate change is predicted to raise both the average summer temperature and the frequency of forest fires. The Arctic mean summer temperature is predicted to increase 2–9 °C by the end of the century (24), and forest fire frequency is expected to at least double per 1 °C rise in temperature (25). Based on the frequency of high BC concentrations (>9 ng $g^{-1}$) reaching the summit of the GIS over the past three centuries (0.015) and the projected change in mean temperature over the next century, we modeled the potential for climate change to alter the surface energy balance over time and change the frequency of widespread melt events on the Greenland Ice Sheet (Fig. 3). Considering only an increase in the surface temperature through the end of the century (in the absence of BC deposition), we can expect the probability of widespread melt to rise to 0.17 or 0.70 for the 2 °C and 9 °C scenarios, respectively. Thus, in the most conservative scenario, by the year 2100, we predict that widespread melting of the surface of the GIS should occur every 6 y on average. When the expected increase in forest fire frequency due to climate change is also included in projections, our simulations suggest that for the 2 °C and 9 °C scenarios, the probability of widespread melt will increase to 0.22 or 0.94, respectively, by the year 2100. Thus, in the least conservative scenario, our projections suggest that the GIS should experience almost annual widespread melting by the year 2100.

This widespread surface melting is likely to alter the surface mass balance of the ice sheet (26). In the dry snow region, retained ice layers generated from the refrozen melt water will further lower the albedo until covered by the next snowfall, and also warm the snowpack upon refreezing. Also, melting can concentrate particles such as BC, which would also lower the surface albedo (27). Therefore, these frequent widespread surface-melting events may initiate a positive feedback mechanism whereby the Greenland Ice Sheet melts even more often than our projections indicate.

In the past, surface melting of the Greenland Ice Sheet over a wide extent including the high, cold, dry snow region occurred only during rare synchronous periods of warm conditions accompanied by high snow surface concentrations of BC. In the future, warmer temperatures and more frequent Northern Hemisphere forest fires driven by climate change may increase the frequency of these widespread melt events, contributing to the further demise of the Greenland Ice Sheet.

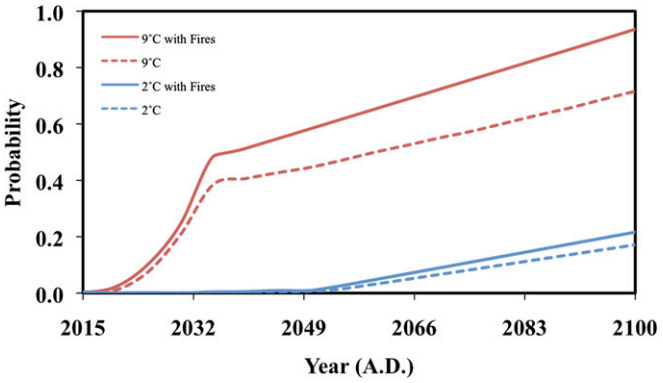


**Fig. 3.** Annual probability of a widespread melt event over the GIS surface from 2015 to 2100 examined over four end-of-century scenarios. In our most conservative projection (2 °C rise in temperature with no change in the frequency of forest fires; blue dotted line), the annual probability of widespread melt should reach 0.17 by the year 2100. In our least conservative projection (9 °C rise in temperature with a twofold increase forest fire frequency per 1 °C increase; red solid line), the annual probability of widespread melt should reach 0.94 by the year 2100.

## Materials and Methods

In each firn core, we used an SP2 intercavity laser-based instrument for measuring BC (with a detection limit of ∼0.02 ng $g^{-1}$) (18), a Picarro L2130-i cavity-ring-down-based laser instrument to measure stable water isotopes ($\delta^{18}O$) (28), and fluorimetry to measure ammonium concentrations (29). For comparison, these records were normalized by the minimum and maximum values in their respective profiles (0.023 ng $g^{-1}$ and 14.4 ng $g^{-1}$ of BC, 0.003 μM and 8.86 μM of ammonium, and −37.6‰ and −30.6‰ $\delta^{18}O$).

The amount of energy needed to generate surface melt and melt water percolation was calculated from the summation of Dingman's equations for the warming phase ($Q_{cc}$), ripening phase ($Q_{m2}$), and output phase ($Q_{m3}$) of melt (30). The amount of energy available at the surface was calculated from a surface energy budget of the top 1 cm of depth by 1 $m^2$ of the snow surface. The projected energy available at the surface was calculated for four possible scenarios over the next 90 y: a 2 °C and 9 °C rise in temperature both with and without an associated rise in forest fire frequency. We calculated the temperature effect on the incoming and outgoing longwave radiation, as well as on the albedo, which decreases from changing microstructure of the warming snowpack (up to −7.5%) (13). We then applied this increase in available energy to a 10-y dataset of daily summer (June 1 to August 31) net radiation. We calculated the effect of BC on the albedo, a 1% reduction when present, by conservatively assuming a doubling in frequency of forest fires per 1 °C rise in temperature (25). In other words, with every 1 °C rise in temperature, we assumed that the probability of a 1% albedo reduction would double. We applied the increase in fire frequency to the 262-y BC record at Summit. At 5-y time steps, we sampled the two energy datasets (temperature effect and BC effect) 1,000 times with replacement using the bootstrapping method; the summation of these two outputs at each time step yielded the projected total surface energy available.

**ACKNOWLEDGMENTS.** We thank the Desert Research Institute ultra-trace ice core chemistry laboratory members, including N. Chellman, L. Layman, O. Maselli, D. Pasteris, and M. Sigl, for their firn core analysis, Z. Courville and Ice Drilling Design and Operations field staff for assistance in collecting the Summit-2010 core, and M. Logan, D. Perovich, M. Borsuk, T. Overly, A. Putman, and M. Ayres for their input. This work was supported by the National Science Foundation (NSF) Arctic Science (ARC) Grant 0806339 and the Dartmouth College Integrative Graduate Education and Research Traineeship Division of Graduate Education Grant 0801490. Analysis of the NEEM core was supported by NSF Office of Polar Programs Grants 0856845 and 0909541. The ACT 3 core was collected and analyzed as part of NASA Grant NAG04GI66G. The Summit 2007 core was collected and analyzed as part of NSF-ARC Grant 0520445.

1. Benson C (1962) Stratigraphic Studies in the Snow and Firn of the Greenland Ice Sheet (US Army Cold Reg Res Lab, Hanover, NH), CRREL Res Rep 70, pp 24–26.
2. Nghiem S, et al. (2012) The extreme melt across the Greenland ice sheet in 2012. *Geophys Res Lett* 39:L20502, 10.1029/2012GL053611.
3. Rennermalm AK, et al. (2013) Understanding Greenland ice sheet hydrology using an integrated multi-scale approach. *Environ Res Lett* 8(1):015017, 10.1088/1748-9326/8/1/015017.
4. Bennartz R, et al. (2013) July 2012 Greenland melt extent enhanced by low-level liquid clouds. *Nature* 496(7443):83–86.
5. Clausen H, Gundestrup N, Johnsen S, Bindschadler R, Zwally J (1988) Glaciological investigations in the Crete area, Central Greenland: A search for a new deep-drilling site. *Ann Glaciol* 10:10–15.
6. Alley R, Koci B (1988) Ice-core analysis at Site A, Greenland: Preliminary results. *Ann Glaciol* 10:1–4.
7. Meese DA, et al. (1994) The accumulation record from the GISP2 core as an indicator of climate change throughout the Holocene. *Science* 266(5191):1680–1682.
8. Fischer H, Werner M, Wagenbach D (1998) Little ice age clearly recorded in northern Greenland ice cores. *Geophys Res Lett* 25(10):1749–1752.
9. Siegenthaler U, Oeschger H (1980) Correlation of $^{18}O$ in precipitation with temperature and altitude. *Nature* 285(5763):314–317.
10. Tedesco M, Serreze M, Fettweis X (2008) Diagnosing the extreme surface melt event over southwestern Greenland in 2007. *Cryosphere* 2(2):159–166.
11. Tedesco M, et al. (2011) The role of albedo and accumulation in the 2010 melting record in Greenland. *Environ Res Lett* 6(1):014005, 10.1088/1748-9326/6/1/014005.
12. Hall D, Williams R, Luthcke S, Digirolamo N (2008) Greenland ice sheet surface temperature, melt and mass loss: 2000–06. *J Glaciol* 54(184):81–93.
13. Tedesco M, et al. (2013) *Greenland Ice Sheet, Arctic Report Card: Update for 2013*. Available at www.arctic.noaa.gov/reportcard/greenland_ice_sheet.html. Accessed December 1, 2013.
14. Flanner M, Zender C (2006) Linking snowpack microphysics and albedo evolution. *J Geophys Res* 111(D12):D12208.
15. Flanner M, Zender C, Randerson J, Rasch P (2007) Present-day climate forcing and response from black carbon in snow. *J Geophys Res* 112(D11):D11202.
16. Warren S, Wiscombe W (1980) A model for the spectral albedo of snow. II: Snow containing atmospheric aerosols. *J Atmos Sci* 37(12):2734–2745.
17. Legrand M, De Angelis M, Staffelbach T, Neftel A, Stauffer B (1992) Large perturbations of ammonium and organic acids content in the Summit-Greenland ice core. Fingerprint from forest fires? *Geophys Res Lett* 19(5):473–475.
18. McConnell JR, et al. (2007) 20$^{th}$-century industrial black carbon emissions altered Arctic climate forcing. *Science* 317(5843):1381–1384.
19. Powell J (1891) *Testimony to Congress: Eleventh Annual Report of the U.S. Geological Survey, 1889–1890, Part 2: Irrigation* (Gov Print Off, Washington, DC), pp 207–208.
20. Barrett S, Arno S, Menakis J (1997) Fires Episodes in the Inland Northwest (1540–1940) Based on Fire History Data (USDA For Serv Intermountain Res Stn, Ogden, Utah) Gen Tech Rep INT-370.
21. Earth Observatory NASA (2012) Smoke and fires in Siberia: Natural hazards. Available at http://earthobservatory.nasa.gov/NaturalHazards/view.php?id=78406&eocn=image&eoci=related_image. Accessed March 13, 2014.
22. NOAA National Climatic Data Center (2012) State of the Climate: Wildfires for June 2012. Available at www.ncdc.noaa.gov/sotc/fire/2012/6. Accessed December 1, 2013.
23. NOAA National Climatic Data Center (2012) State of the Climate: Wildfires for July 2012. Available at www.ncdc.noaa.gov/sotc/fire/2012/7. Accessed December 1, 2013.
24. Intergovernmental Panel on Climate Change (2013) *IPCC Fifth Assessment Report, Climate Change 2013: The Physical Science Basis* (Cambridge Univ. Press, Cambridge).
25. Westerling AL, Hidalgo HG, Cayan DR, Swetnam TW (2006) Warming and earlier spring increase western U.S. forest wildfire activity. *Science* 313(5789):940–943.
26. Van Angelen J, et al. (2012) Sensitivity of Greenland Ice Sheet surface mass balance to surface albedo parameterization: A study with a regional climate model. *The Cryosphere* 6(5):1175–1186.
27. Doherty SJ, et al. (2013) Observed vertical redistribution of black carbon and other insoluble light-absorbing particles in melting snow. *J Geophys Res* 118(11):5553–5569.
28. Maselli OJ, Fritzsche D, Layman L, McConnell JR, Meyer H (2013) Comparison of water isotope-ratio determinations using two cavity ring-down instruments and classical mass spectrometry in continuous ice-core analysis. *Isotopes Environ Health Stud* 49(3):387–398.
29. McConnell JR, Lamorey GW, Lambert SW, Taylor KC (2002) Continuous ice-core chemical analyses using inductively coupled plasma mass spectrometry. *Environ Sci Technol* 36(1):7–11.
30. Dingman L (1994) *Physical Hydrology* (Prentice Hall, Englewood Cliffs, NJ).